

*Original Research Article*

# Unleashing the Power of Oxygen-Doped Graphitic Carbon Nitride: Enhancing Neutral Red Removal Efficiency

**Muchammad Tamyiz<sup>1\*</sup>, Maulana Ahmad Annafis<sup>1</sup>, Ahza Refkyan Dhafa<sup>1</sup>, Muhammad Basir Chis Bulloh<sup>1</sup>, Mohd Hanif Mohd Pital<sup>2,3</sup>**<sup>1</sup>Department of Environmental Engineering, Faculty of Engineering, Universitas Nahdlatul Ulama Sidoarjo, Jalan Lingkar Luar, Rangkah Kidul, Sidoarjo, Jawa Timur, Indonesia 61234<sup>2</sup>Faculty of Chemical Engineering & Technology, Universiti Malaysia Perlis (UniMAP), 02600 Arau, Perlis, Malaysia<sup>3</sup>Centre of Excellence for Biomass Utilization, Universiti Malaysia Perlis (UniMAP), 02600 Arau, Perlis, Malaysia\* Corresponding Author, email: [mtamyiz.tkl@unusida.ac.id](mailto:mtamyiz.tkl@unusida.ac.id)

---

## Abstract

Textile industry wastewater often contains persistent pollutants like neutral red dye, which are challenging to break down and harmful to ecosystems. This study introduces oxygen-doped graphitic carbon nitride (O-g-C<sub>3</sub>N<sub>4</sub>) as a photocatalyst to degrade neutral red dye under visible light. Synthesized using a single-step calcination of urea, dicyandiamide, and oxalic acid, O-g-C<sub>3</sub>N<sub>4</sub> was tested for its efficiency in neutral red removal through adsorption and photocatalytic degradation, both in light and dark conditions. Results showed that O-g-C<sub>3</sub>N<sub>4</sub> quickly adsorbed the dye, reaching equilibrium in 30 minutes and achieving a maximum adsorption capacity of 1.86 mg g<sup>-1</sup>, surpassing bulk g-C<sub>3</sub>N<sub>4</sub>. Kinetic analysis indicated that adsorption followed a pseudo-second-order model, suggesting chemisorption as the primary mechanism. Under visible light, O-g-C<sub>3</sub>N<sub>4</sub>'s photocatalytic degradation reached 86% neutral red removal, compared to 51% with bulk g-C<sub>3</sub>N<sub>4</sub>, largely due to improved light absorption and reduced electron-hole recombination. Degradation of neutral red followed pseudo-first-order kinetics, with O-g-C<sub>3</sub>N<sub>4</sub>'s reaction rate three times greater than bulk g-C<sub>3</sub>N<sub>4</sub>. The Sips isotherm best fit the adsorption data, confirming heterogeneous active sites and multilayer adsorption. These findings highlight O-g-C<sub>3</sub>N<sub>4</sub>'s potential for environmental remediation.

**Keywords:** Adsorption; g-C<sub>3</sub>N<sub>4</sub>; heterogeneous; neutral red; photocatalysis

---

## 1. Introduction

Artificial dyes are extensively used across various industries, including textiles, paper, and leather, to provide long-lasting colors to products (Zhu et al., 2024; Gholivand et al., 2015; Somnath et al., 2022). These dyes often consist of complex organic molecules with substituted sites or linkages (Gholivand et al., 2015). When exposed to environmental conditions, the effluent discharged from these industries, which contains dye molecules, poses a significant risk to both living organisms and aquatic ecosystems—vital sources of life for all species (Khan et al., 2024). Due to the water-soluble nature of most dyes, their removal from wastewater through conventional methods is challenging. Neutral red, an aromatic heterocyclic cationic dye, while having low toxicity, is harmful due to its poor biodegradability and intense dyeing properties. The presence of neutral red in wastewater can decrease light penetration, thereby hindering photosynthesis in aquatic plants, and it also exhibits toxic effects on microbial populations, severely damaging the aquatic environment (Yan et al., 2014; Sadia et al., 2021; Liu et al., 2023). The decomposition of neutral red at high temperatures may result in the production of dangerous

by-products, and it is associated with adverse effects such as carcinogenicity and chronic toxicity (Sadia et al., 2021). Many dyes are chemically stable and resistant to degradation, making traditional physical and biological treatment methods ineffective (Shahid et al., 2021). Consequently, the efficient removal of complex organic dyes, both cationic and anionic, continues to be a key focus of research worldwide.

Semiconductor photocatalysis has become a promising approach for effective water purification (Liang et al., 2025). Titanium dioxide (TiO<sub>2</sub>) remains the most extensively researched semiconductor material due to its high photocatalytic activity under ultraviolet (UV) light (Zhu et al., 2024). However, since UV light makes up only 2–3% of sunlight, its effectiveness in real-world applications, particularly for environmental remediation under natural light, is significantly limited. Therefore, developing new photocatalysts that can be driven by visible light is of great importance (Xie et al., 2020). Graphitic carbon nitride (g-C<sub>3</sub>N<sub>4</sub>), an organic polymer, is one such material, has garnered significant attention because its outstanding physical and chemical characteristic, including costless, high thermal stability, lack of toxicity, and a suitable electronic band structure (Tamyiz and Doong, 2023; Tamyiz et al., 2023). These features have led to its wide use in environmental decontamination and energy conversion, including the emerging pollutants degradation, hydrogen evolution, and reduction of carbon dioxide. Despite its advantages, bulk g-C<sub>3</sub>N<sub>4</sub> faces several limitations, such as fast electron-hole recombination, low quantum efficiency, and a limited specific surface area, which restrict its practical use (Xie et al., 2020). To enhance its photocatalytic performance, various modifications have been made, such as the deposition of noble metal nanoparticles, heterojunction construction, element doping, morphology control, and the introduction of defects (Liang et al., 2025). These modifications have resulted in enhanced photocatalytic efficiency compared to bulk g-C<sub>3</sub>N<sub>4</sub>. Among various modification techniques, heteroatom doping is regarded as one of the most effective methods. Adding heteroatoms to g-C<sub>3</sub>N<sub>4</sub> has been shown to modify its electron structure and bandgap, greatly boosting catalytic efficiency. Doping with heteroatoms such as boron, fluorine, phosphorus, and sulfur is a widely recognized approach to adjust the surface electronic properties of g-C<sub>3</sub>N<sub>4</sub>, thereby enhancing its catalytic performance (Liu et al., 2021).

Among these, element doping has proven to be particularly effective (Husein et al., 2024). The incorporation of doping elements into g-C<sub>3</sub>N<sub>4</sub> leads to changes in its electronic structure, such as narrowing the band gap and expanding the light absorption range. These modifications enhance its ability to harness visible light more effectively (Zhang et al., 2024). For instance, Gupta et al. (2020) created S-doped g-C<sub>3</sub>N<sub>4</sub> photocatalysts using materials like thiourea and successfully reduced band gap of 2.64 eV (Gupta et al., 2020). Furthermore, Li et al. demonstrated that phosphorous-doped g-C<sub>3</sub>N<sub>4</sub> has a reduced band gap of 2.42 eV (smaller than the 2.63 eV band gap of bulk g-C<sub>3</sub>N<sub>4</sub>) using combination materials like hexachlorotriphosphazene and melamine. Phosphorous doping introduces defects in the structure of g-C<sub>3</sub>N<sub>4</sub>, which enhances photocatalytic performance by capturing photo-generated electrons, promoting charge transfer, inhibiting electron-hole recombination, and prolonging charge carrier lifetimes. Additionally, sulfur and phosphorus co-doped g-C<sub>3</sub>N<sub>4</sub> have shown a 4-fold increase in rhodamine B decomposition activity (Li et al., 2020). In this research, we present a simple and efficient approach for synthesizing oxygen-doped g-C<sub>3</sub>N<sub>4</sub> by calcining a mixture of two precursors, dicyandiamide and urea, in the presence of oxalic acid for degradation of neutral red. The neutral red removal efficiency from aqueous solutions was also evaluated through adsorption and photocatalytic degradation under both light and dark conditions.

## 2. Methods

This research is an experimental laboratory study using a quantitative approach. Oxygen-doped g-C<sub>3</sub>N<sub>4</sub> was synthesized in a sustainable process through the calcination of urea, dicyandiamide, and oxalic acid.

### 2.1. Materials and Reagents

All the chemical reagents employed in this research were of analytical grade, and deionized water (DI) was utilized throughout the experimental procedures. Analytical grade chemicals are used in

experimental research to ensure high levels of purity, accuracy, reliability, and avoid unexpected reactions in results. The chemicals employed included urea ( $\text{CH}_4\text{N}_2\text{O}$ ), dicyandiamide ( $\text{C}_2\text{H}_4\text{N}_4$ ), Neutral Red ( $\text{C}_{15}\text{H}_{17}\text{CIN}_4$ ), oxalic acid ( $\text{C}_2\text{H}_2\text{O}_4$ ), ethanol ( $\text{C}_2\text{H}_6\text{O}$ ), acetone ( $\text{CH}_3\text{COCH}_3$ ), methanol ( $\text{CH}_3\text{OH}$ ), isopropyl alcohol ( $\text{C}_3\text{H}_8\text{O}$ ), and sulfuric acid ( $\text{H}_2\text{SO}_4$ ), all of which were of analytical grade.

## 2.2. Synthesis of g- $\text{C}_3\text{N}_4$

The g- $\text{C}_3\text{N}_4$  was synthesized through the thermal polycondensation method. Specifically, 4 grams of urea and 2 grams of dicyandiamide, and then ground together to produce smooth powder. As previous our experiment, a covered crucible was used to facilitate the calcination of the powdered sample at  $550^\circ\text{C}$  for 4 hours at a rate of  $4^\circ\text{C}$  per minute, then left to cool naturally (Tamyiz and Doong, 2023). The resulting yellow powder was ground and rinsed three times using deionized water and ethanol, and subsequently dried.

## 2.3. Synthesis of oxygen-doped g- $\text{C}_3\text{N}_4$

The preparation of O-g- $\text{C}_3\text{N}_4$  through one-pot calcination method involved mixing 4 grams of urea, 2 grams of dicyandiamide, and 0.6 grams of oxalic acid, and then grinding the mixture in an agate mortar for 30 minutes to ensure all material were mixed. The ground white powder was positioned inside a muffle furnace, heated at  $550^\circ\text{C}$  for 4 hours in an air atmosphere, and then allowed to cool naturally (Tamyiz et al., 2023). After cooling, the product was ground again using an agate mortar.

## 2.4. Evaluation of Photocatalytic Performance

A handmade photoreactor was employed for the photocatalysis experiments, with low power LED lamp (80-watt) serving as the visible light source. To begin, 10 mg of the prepared sample was weighed and combined with 10 mL of the neutral red solution in the photoreactor cell. The solution was blended in the absence of light for 30 minutes to enable the sample to reach adsorption equilibrium, ensuring that adsorption did not interfere with the photocatalysis results. In order to characterize the dynamics of neutral red adsorption on oxygen doped g- $\text{C}_3\text{N}_4$ , the kinetic models of pseudo-first-order (PFO) and pseudo-second-order (Psomopoulos et al.) reactions were employed. Furthermore, to explore the adsorption mechanism of the photocatalytic adsorbent in more depth, the Langmuir, Freundlich, and Temkin isotherm models were used. After the 30-minute dark phase, the LED lamp was switched on. At 10-minute intervals, 2 mL of the reaction solution was drawn using a pipette and placed into a centrifuge tube, then centrifuged at 7000 RPM till separated well. The wavelength of the supernatant was determined using a B-One UV-Vis spectrophotometer. The photocatalytic efficiency was determined using the equation below (1):

$$\eta = \frac{A_0 - A_t}{A_0} \times 100 \quad (1)$$

In this equation,  $\eta$  denotes the efficiency of photocatalytic degradation,  $A_0$  refers to the initial absorbance of the neutral red solution, and  $A_t$  represents the absorbance at a specific time (t) during the photocatalytic degradation process (Gholivand et al., 2015). The The neutral red photodegradation follows first-order kinetics, that can be formulated by the following equation (2):

$$\ln \frac{C_0}{C_t} = k \quad (2)$$

In this equation,  $C_0$  represents the initial neutral red concentration,  $C_t$  is the concentration at time t during the photocatalytic process,  $k$  stands for the rate constant of the photodegradation, and t refers to the duration of the photocatalytic reaction.

## 3. Result and Discussion

The study examined the synergistic effects of adsorption and photocatalytic degradation of neutral red (NR) using oxygen-doped graphitic carbon nitride (OCN) under both light and dark conditions. The primary aim was to assess the contribution of adsorption by conducting experiments in

the dark, thereby excluding the influence of photocatalysis. In this way, the data would reflect adsorption as the sole mechanism for the neutral red elimination from the solution. The adsorption studies were executed using a 10 mg L<sup>-1</sup> neutral red concentration solution, prepared at neutral pH (pH 7), with 1.0 g L<sup>-1</sup> of the synthesized oxygen-doped g-C<sub>3</sub>N<sub>4</sub> samples (Gholivand et al., 2015). These conditions were maintained to focus on the adsorption process without interference from light-driven photocatalytic activity. The findings revealed that equilibrium and saturation of adsorption were reached within 30 minutes, with the bulk of the adsorption occurring in the first 10 minutes. Following this rapid initial adsorption phase, the rate slowed down until equilibrium was reached. A maximum adsorption capacity of 1.86 mg g<sup>-1</sup> was observed for the oxygen-doped g-C<sub>3</sub>N<sub>4</sub>, which was significantly higher compared to the bulk g-C<sub>3</sub>N<sub>4</sub>, which demonstrated an adsorptive capacity of only 0.93 mg g<sup>-1</sup> (Figure 1a). In terms of removal efficiency, oxygen-doped g-C<sub>3</sub>N<sub>4</sub> showed a 17% removal of neutral red, while bulk g-C<sub>3</sub>N<sub>4</sub> only achieved 9% removal (Figure 1b). This marked difference in adsorption capacities and removal efficiencies highlights the enhancement in performance because the oxygen doping of the g-C<sub>3</sub>N<sub>4</sub>. The doping likely improved the surface area or created additional active sites for adsorption, thus boosting the adsorbent's ability to capture neutral red dye (Liang et al., 2025).

The rapid adsorption observed in the first 10 minutes indicates that the oxygen-doped g-C<sub>3</sub>N<sub>4</sub> has a high affinity for neutral red, as the adsorption capacity reached 1.55 mg g<sup>-1</sup> in this short time. However, after the initial rapid uptake, the adsorption rate began to slow, and by the 30-minute mark, the system had reached equilibrium, meaning that no further adsorption occurred. This pattern is common in many adsorption systems, where a rapid initial phase is followed by a slower progression towards equilibrium as the adsorption sites on the surface of the adsorbent become increasingly saturated. The performance of oxygen-doped g-C<sub>3</sub>N<sub>4</sub> in adsorbing neutral red from the solution can be attributed to several factors. First, the integration of oxygen into the g-C<sub>3</sub>N<sub>4</sub> skeleton may have altered its electronic structures, improving its interaction with the dye molecules. Moreover, the oxygen-doped g-C<sub>3</sub>N<sub>4</sub> structure likely provided a larger surface area compared to bulk g-C<sub>3</sub>N<sub>4</sub>, increasing the adsorption sites number. This result shows the significant factor in the adsorption of neutral red molecules (Gholivand et al., 2015). The rapid initial adsorption rate reflects the strong affinity between the neutral red molecules and the oxygen-doped g-C<sub>3</sub>N<sub>4</sub>. However, the gradual decrease in rate as equilibrium approaches indicates that once the easily accessible sites are occupied, further adsorption is constrained by the limited availability of remaining active sites.

**Table 1.** Isotherm and kinetic model result of oxygen-doped g-C<sub>3</sub>N<sub>4</sub>.

Model	Parameter	Value	R <sup>2</sup>
Isotherm			
Langmuir	q <sub>m</sub> (mg g <sup>-1</sup> )	9.64	0.968
	K <sub>L</sub> (L mg <sup>-1</sup> )	0.02	
Fruendlich	K <sub>F</sub> ((mg g <sup>-1</sup> )/(L mg <sup>-1</sup> ) <sup>1/n</sup> )	0.23	0.959
	1 n <sup>-1</sup>	1.24	
Sips	q <sub>m</sub> (mg g <sup>-1</sup> )	4.39	0.978
	K <sub>S</sub> (L mg <sup>-1</sup> )	0.07	
	γ	1.54	
Kinetic			
Pseudo-first-order	K <sub>i</sub> (min <sup>-1</sup> )	0.26	0.993
	q <sub>e</sub> (mg g <sup>-1</sup> )	1.68	
Pseudo-second-order	K <sub>2</sub> (g (mg·min) <sup>-1</sup> )	0.22	0.999
	q <sub>e</sub> (mg g <sup>-1</sup> )	1.86	

In this research, the adsorption characteristic of neutral red molecules onto oxygen-doped g-C<sub>3</sub>N<sub>4</sub> was also evaluated using kinetic models to better understand the underlying mechanisms. Two

commonly utilized kinetic models were applied: the pseudo-1<sup>st</sup>-order and pseudo-2<sup>nd</sup>-order kinetic models. The kinetic modeling allows for an assessment of how the adsorption process progresses over time and helps identify the dominant factors influencing adsorption rates. The adsorption process demonstrated a rapid initial uptake of the neutral red molecules, which gradually slowed down after 10 minutes and ultimately reached equilibrium at 30 minutes. This quick adsorption phase is largely attributed to the distinctive properties of the oxygen-doped g-C<sub>3</sub>N<sub>4</sub> material, specifically its mesoporous structure. Mesoporous are pores with diameters between 2 and 50 nanometers, which play a critical role in facilitating the diffusion of adsorbates like neutral red molecules into the material. In this case, the mesoporous structure likely provided easy access for the neutral red molecules, enabling a swift adsorption rate during the initial phase. However, as time passed and the adsorption sites reached saturation, the adsorption rate decreased until equilibrium was achieved.

To understand the adsorption study, the experimental data were examined using both the pseudo-1<sup>st</sup>-order and pseudo-2<sup>nd</sup>-order models, and the fitting curves were depicted in (Figure 1c). The primary distinction between these two models lies in their underlying assumptions about the step that controls the overall rate of the adsorptive behavior. The pseudo-1<sup>st</sup>-order model posits that the rate of adsorption has a direct correlation to the number of available adsorption sites, while the pseudo-2<sup>nd</sup>-order model suggests that the rate is directly related to the square of the quantity of available sites.

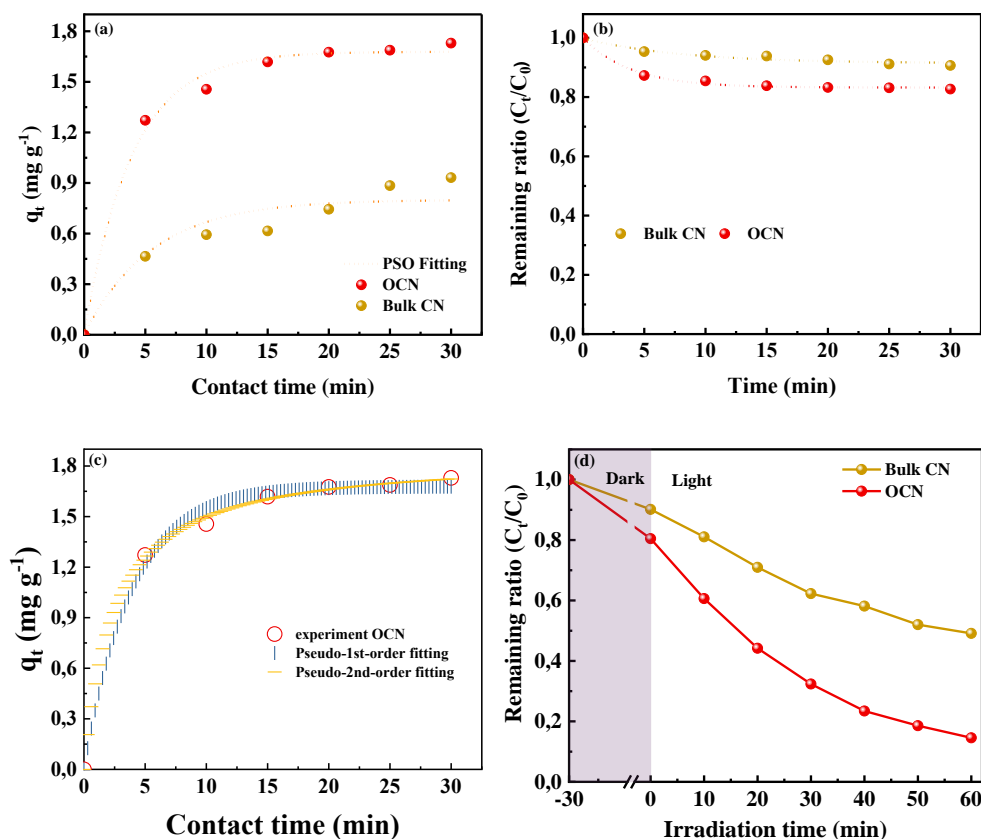


**Figure 1.** (a-b) The pseudo-2<sup>nd</sup>-order fitting and the bulk g-C<sub>3</sub>N<sub>4</sub> and oxygen-doped g-C<sub>3</sub>N<sub>4</sub> adsorption equilibrium, (c) the pseudo-1<sup>st</sup>-order and pseudo-2<sup>nd</sup>-order kinetic models of oxygen-doped g-C<sub>3</sub>N<sub>4</sub>, and (d) photodegradation of neutral red under visible light.

Table 1 provides a detailed comparison of the parameters derived from the two models. The analysis described that the pseudo-2<sup>nd</sup>-order model offered a more accurate fit to the experimental data, with a higher coefficient of determination ( $R^2 = 0.999$ ) in comparison to the pseudo-1<sup>st</sup>-order model ( $R^2 = 0.993$ ). This represents that the pseudo-2<sup>nd</sup>-order model more precisely reflects the adsorption kinetics in this system. The high  $R^2$  value for the pseudo-2<sup>nd</sup>-order model implies that the adsorption kinetics is

likely dominated by chemisorption rather than physisorption. Chemisorption entails the formation of stronger chemical bonds, like covalent or ionic bonds, between the adsorbate and adsorbent, while physisorption generally involves weaker van der Waals forces. The pseudo-2<sup>nd</sup>-order model's assumption that the rate of adsorption is proportional to the square of the quantity of unoccupied sites suggests that electron sharing or transfer may have a substantial impact on the adsorption mechanism. The result aligns well with the observed changes in the surface chemistry of the material before and after adsorption. In particular, chemisorption often involves the exchange or sharing of electrons between the adsorbent and the adsorbate, which could explain the stronger binding observed in this study.

The strong agreement between the pseudo-2<sup>nd</sup>-order model and the experimental results suggests that the neutral red molecules adsorption onto oxygen-doped g-C<sub>3</sub>N<sub>4</sub> is predominantly a chemically driven process (Li et al., 2020). This conclusion is further supported by the material's mesoporous structure, which not only enhances the diffusion of adsorbate molecules but also provides an environment conducive to chemical interactions. Such findings are valuable for the design of adsorbent materials in environmental and industrial applications, where efficient adsorption and strong chemical binding are critical for removing contaminants or recovering valuable compounds from aqueous solutions. In the next experiment, bulk g-C<sub>3</sub>N<sub>4</sub> and oxygen-doped g-C<sub>3</sub>N<sub>4</sub> were tested under visible light for their ability to degrade neutral red. After 60 minutes of exposure, the g-C<sub>3</sub>N<sub>4</sub> showed a 51% removal of the dye, while the oxygen-doped g-C<sub>3</sub>N<sub>4</sub> demonstrated a considerably higher removal efficiency of 86%. (Figure 1d). The significant improvement in performance is credited to the alterations introduced by incorporating oxygen into the g-C<sub>3</sub>N<sub>4</sub> structure. Oxygen doping improves the capacity of photocatalyst to absorb visible light and plays a key role in lowering the electron-hole pairs recombination rate (e<sup>-</sup>-h<sup>+</sup> pairs). The reduced recombination rate is crucial for improving the overall photocatalytic efficiency process, as more electron-hole pairs are available to initiate and sustain chemical reactions responsible for degrading pollutants (Liang et al., 2025).

The degradation of neutral red was found to follow pseudo-1<sup>st</sup>-order kinetics, a common behavior observed in many photocatalytic reactions. In this context, the oxygen-doped g-C<sub>3</sub>N<sub>4</sub> demonstrated enhanced performance resulting from a combined effect of adsorption and photocatalysis. One of the key reasons behind this enhanced performance is the structural characteristics of oxygen-doped g-C<sub>3</sub>N<sub>4</sub>. The material is designed with a mesoporous structure, providing a large surface area that allows more effective adsorption of neutral red molecules onto the surface of oxygen-doped g-C<sub>3</sub>N<sub>4</sub>. The neutral red molecules adsorption in the oxygen-doped g-C<sub>3</sub>N<sub>4</sub> is critical, as it concentrates the dye molecules near the active sites, facilitating more efficient interactions between the dye and the photocatalyst. Once the neutral red are adsorbed on the surface, oxygen-doped g-C<sub>3</sub>N<sub>4</sub> uses visible light to excite electrons, creating electron-hole pairs. These pairs trigger reactions that result in the reactive oxygen species (ROS) formation, such as •O<sub>2</sub><sup>-</sup> (superoxide radicals) and •OH (hydroxyl radicals) (Wang et al., 2024). These ROS are highly reactive and play a main role in breaking down dye molecules like neutral red into smaller, less harmful components. The more effective production of ROS in oxygen-doped g-C<sub>3</sub>N<sub>4</sub> further clarifies its improved photodegradation activity in comparison to undoped g-C<sub>3</sub>N<sub>4</sub>.

The kinetic behavior of the two photocatalysts were assessed by determining their reaction rate constants. For g-C<sub>3</sub>N<sub>4</sub>, the rate constant was determined to be 0.0104 min<sup>-1</sup>, while the rate constant of oxygen-doped g-C<sub>3</sub>N<sub>4</sub> was markedly higher at 0.0290 min<sup>-1</sup> (Figure 2a). This threefold increase in the reaction rate clearly demonstrates the superior efficiency of oxygen-doped g-C<sub>3</sub>N<sub>4</sub> in photocatalytic applications. The faster reaction rate indicates that the oxygen-doped version can degrade neutral red much more quickly, making it a more viable option for large-scale water purification and pollutant removal systems. Several factors contribute to the improved performance of oxygen-doped g-C<sub>3</sub>N<sub>4</sub>. First, the process of doping embeds extra energy levels into the band structure of the material. The introduction of these new energy levels helps the material absorb more visible light, thus facilitating the use of more photons to excite electrons and produce critical electron-hole pairs (Mishra et al., 2024). Second, The oxygen atoms embedded within the g-C<sub>3</sub>N<sub>4</sub> structure act as electron traps, which inhibit the

recombination of electron-hole pairs and prolong their lifespan. The prolonged lifetime enables more effective use of charge carriers in photocatalytic reactions.

In contrast, bulk g-C<sub>3</sub>N<sub>4</sub> tends to exhibit a faster electron-hole recombination rate, which restricts its photocatalytic efficiency. When electron-hole pairs recombine quickly, they do not have sufficient time to participate in chemical reactions, thus reducing the overall effectiveness of the photocatalytic process. Oxygen doping mitigates this issue, leading to a material that is not only more responsive to visible light but also more efficient in sustaining the photocatalytic reactions needed for pollutant degradation. The large surface area and mesoporous structure of oxygen-doped g-C<sub>3</sub>N<sub>4</sub> also contribute to its enhanced performance. A mesoporous structure is advantageous in photocatalysis because it provides numerous active sites where the reactions can occur (Mishra et al., 2024). Moreover, the large surface area increases the likelihood of dye molecules like neutral red coming into contact with the photocatalyst, which is critical for initiating the degradation process. The combination of these factors, which is improved light absorption, reduced recombination, and an optimized structure, makes oxygen-doped g-C<sub>3</sub>N<sub>4</sub> a highly effective material for environmental cleanup applications.

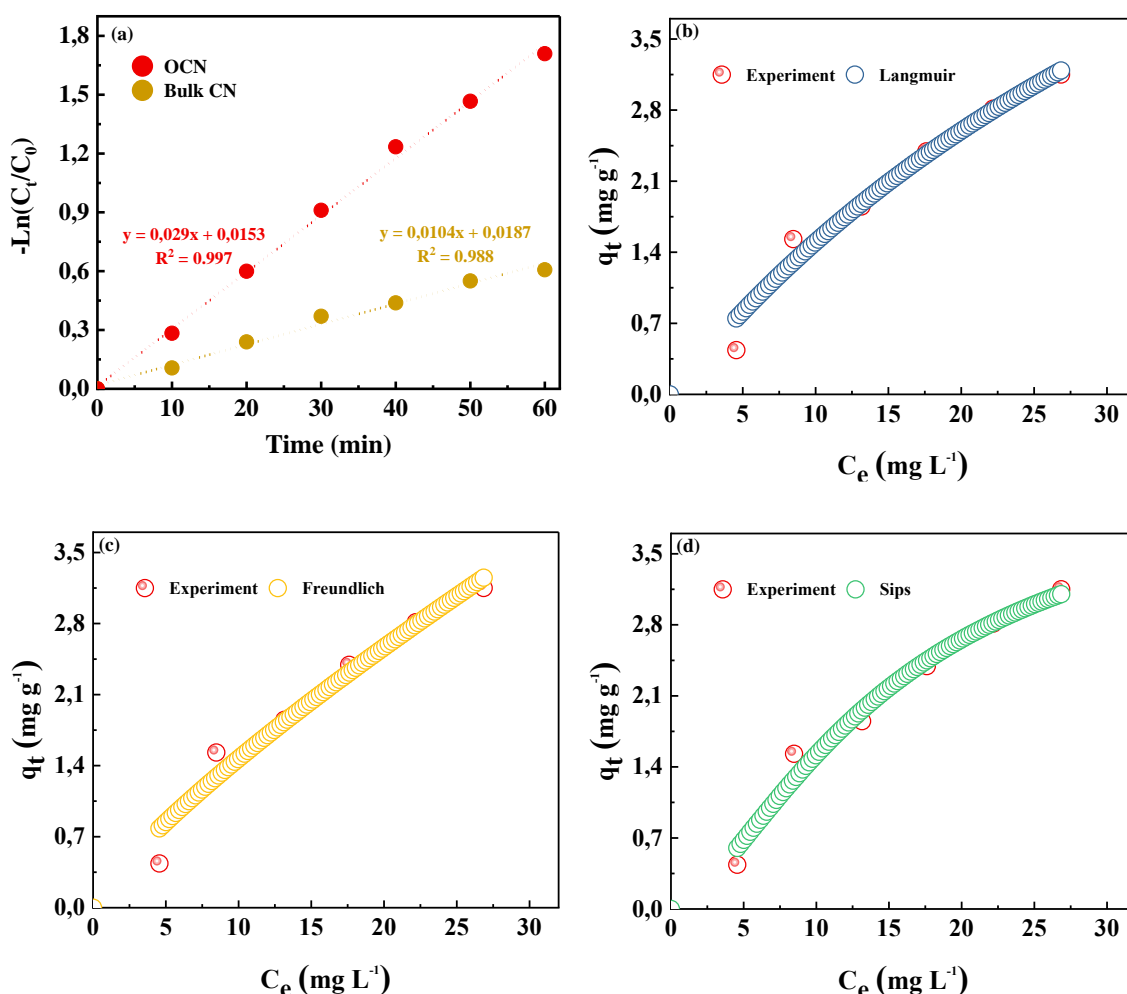
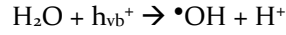


**Figure 2.** (a) The reaction rate constants for g-C<sub>3</sub>N<sub>4</sub> and oxygen-doped g-C<sub>3</sub>N<sub>4</sub> upon neutral red photodegradation, the isotherm models (b) Langmuir, (c) Freundlich, and (d) Sips.

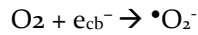
The reaction mechanism of neutral red degradation through the following photocatalytic process, under visible light exposure, oxygen-doped g-C<sub>3</sub>N<sub>4</sub> promotes electrons from its valence band to the conduction band (Mishra et al., 2024), resulting in the formation of an electron-hole pair:



Here,  $e_{cb}^-$  indicates the electron located in the conduction band, while  $h_{vb}^+$  symbolizes the electron vacancy within the valence band. Both of these species can move to the surface of photocatalyst, where they participate in redox reactions with other species that are attached to the surface (Mishra et al., 2024). Typically, surface-bound water can readily react with  $h_{vb}^+$ , resulting in the production of hydroxyl radicals ( $\bullet\text{OH}$ ):

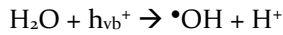


The extremely reactive hydroxyl radicals ( $\bullet\text{OH}$ ) are vital for the photodegradation process of neutral red molecules. Simultaneously, the interaction between conduction band electrons and oxygen molecules generates superoxide radicals ( $\bullet\text{O}_2^-$ ) (Mishra et al., 2024):

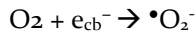


The hydroxyl radicals ( $\bullet\text{OH}$ ) and superoxide radicals ( $\bullet\text{O}_2^-$ ) produced during the photocatalytic process are responsible for degrading the neutral red molecules into less harmful byproducts. This process can be represented by the following reactions:

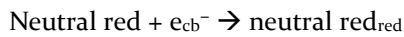
- (1) Generation of hydroxyl radicals:



- (2) Generation of superoxide radicals:



- (3) Degradation of neutral red by oxygen species:



Adsorption is a critical mechanism for various environmental and industrial processes, especially when it comes to removing pollutants from aqueous solutions. In this context, understanding how adsorption works at the molecular level can enhance the efficiency of adsorbents and the removal of contaminants. In order to gain a clearer insight into the adsorption process, three isotherm models were utilized: Langmuir, Freundlich, and Sips, and their non-linear fits were analyzed to identify the best model to describe neutral red adsorption onto oxygen-doped  $\text{g-C}_3\text{N}_4$ . Adsorption isotherms are mathematical models that describe how adsorbates (in this case, Neutral Red) interact with the adsorbent (oxygen-doped  $\text{g-C}_3\text{N}_4$ ) at equilibrium. By understanding the adsorption behavior through these models, researchers can assess the efficiency and potential of an adsorbent for practical applications. In this study, the experimental data were analyzed using the Langmuir, Freundlich, and Sips isotherms, with the parameters presented in Table 1 and non-linear fits shown in (Figures 2b-d). Each model represents different assumptions about the adsorption process, offering a deeper insight into how oxygen-doped  $\text{g-C}_3\text{N}_4$  interacts with neutral red.

The Sips isotherm served the model that best fits the experimental data is indicated by an  $R^2$  value of 0.978, followed by the Langmuir model with an  $R^2$  of 0.968 and the Freundlich model with an  $R^2$  of 0.959. The significant  $R^2$  value for the Sips model suggests that it best captures the adsorption dynamics of neutral red on oxygen-doped  $\text{g-C}_3\text{N}_4$ , making it a suitable model for predicting adsorption capacity and kinetics. As a hybrid isotherm, the Sips model integrates aspects of the Langmuir and Freundlich models, rendering it particularly suitable for describing systems that exhibit heterogeneous surfaces and multilayer adsorption, which is often the case with modified materials like oxygen-doped  $\text{g-C}_3\text{N}_4$ .

According to the Langmuir model, adsorption occurs on a homogeneous surface that contains a fixed number of equivalent adsorption sites, leading to monolayer adsorption. This model is appropriate for systems in which each adsorption site exhibits the same affinity for the adsorbate, and interactions between the adsorbed molecules are absent. Despite its simplicity, the Langmuir model fit the data relatively well, with an  $R^2$  value of 0.968. The relatively high  $R^2$  value indicates that a significant portion of the adsorption process on oxygen-doped g-C<sub>3</sub>N<sub>4</sub> may follow a monolayer adsorption mechanism, particularly at lower concentrations of neutral red. This model also assumes that once an adsorption site is filled, no additional adsorption can occur at that site, which may explain its limited applicability at higher concentrations of the dye.

In contrast, the Freundlich isotherm characterizes adsorption on a surface that is heterogeneous, where adsorption sites have varying affinities for the adsorbate. This model is more flexible than the Langmuir isotherm, as it allows for multilayer adsorption and does not assume uniform adsorption energy across the surface. The Freundlich model fit the data with an  $R^2$  value of 0.959, which is slightly lower than that of the Langmuir model. This implies that while the Freundlich model accounts for some of the surface heterogeneity of oxygen-doped g-C<sub>3</sub>N<sub>4</sub>, it may not fully represent the complexity of the adsorption process, particularly at higher concentrations where interactions between adsorbed molecules become more significant. Known as the Langmuir-Freundlich isotherm, the Sips model integrates aspects of both the Langmuir and Freundlich models. This hybrid model is particularly useful for describing systems that exhibit both homogenous and heterogeneous adsorption behavior, as well as multilayer adsorption. With an  $R^2$  value of 0.978, the Sips model offered the most accurate fit to the experimental data, suggesting it reliably describes the adsorption of neutral red on oxygen-doped g-C<sub>3</sub>N<sub>4</sub>. The ability of the Sips model to account for surface heterogeneity and multilayer adsorption makes it an ideal choice for systems involving modified adsorbents like oxygen-doped g-C<sub>3</sub>N<sub>4</sub>, which often possess a complex surface structure due to oxygen doping and other surface modifications of the g-C<sub>3</sub>N<sub>4</sub>.

An important parameter derived from the Sips model is the maximum adsorption capacity,  $q_m$ , which was determined to be 4.39 mg/g for the adsorption of neutral red on oxygen-doped g-C<sub>3</sub>N<sub>4</sub>. This value signifies the maximum capacity for neutral red adsorption on the adsorbent's surface given the current experimental conditions. The relatively high adsorption capacity suggests that oxygen-doped g-C<sub>3</sub>N<sub>4</sub> is an effective adsorbent for neutral red, particularly at higher initial concentrations. The increase in adsorption with higher equilibrium concentrations ( $C_e$ ) further supports this conclusion, as it indicates that the adsorbent can capture more dye molecules as the concentration of neutral red in the solution increases. In addition to the  $q_m$  value, the Sips model also provides insight into the nature of the adsorption process through its  $\gamma$  parameter, which was found to be 1.54 (Zhou et al., 2020). The  $\gamma$  value is a significant indicator of the adsorption mechanism, as it implies that the adsorption process involves interactions among the adsorbed neutral red molecules. This is consistent with a multilayer adsorption process, where adsorbed molecules can form additional layers on top of the initial adsorbate layer. The presence of multilayer adsorption is further supported by the L<sub>2</sub>-type isotherm observed for oxygen-doped g-C<sub>3</sub>N<sub>4</sub>, which indicates a high degree of attraction between the adsorbent and the adsorbate, likely facilitated by chemical bonding or electrostatic interactions (Abbasi et al., 2022). The chemical bonds or electrostatic interactions that take place during the adsorption process are particularly important for understanding the adsorption mechanism of oxygen-doped g-C<sub>3</sub>N<sub>4</sub> (Xu et al., 2025). By doping with oxygen, extra functional groups are incorporated onto the surface of g-C<sub>3</sub>N<sub>4</sub>, which can enhance its interaction with organic molecules like neutral red. These functional groups can form hydrogen bonds or engage in electrostatic interactions with the dye molecules, leading to a stronger adsorption affinity (Xu et al., 2025). The existence of these interactions is evidenced by the high adsorption capacity noted in the study, along with the L<sub>2</sub>-type isotherm, which is typical of systems exhibiting strong interactions between the adsorbate and adsorbent (Abbasi et al., 2022).

The embedding of oxygen atoms within the g-C<sub>3</sub>N<sub>4</sub> structure also results in a more heterogeneous surface, with a wider range of adsorption energies. The Sips model reflects this heterogeneity by

accommodating both high-energy and low-energy adsorption sites. The high-energy sites are likely associated with the oxygen functional groups, which have a strong affinity for neutral red, while the low-energy sites may be associated with the undoped regions of the g-C<sub>3</sub>N<sub>4</sub> surface. The combination of these high- and low-energy sites contributes to the overall adsorptive capacity of oxygen-doped g-C<sub>3</sub>N<sub>4</sub>, as it allows the material to adsorb dye molecules across a wide range of concentrations (Mishra et al., 2024). The significant adsorption affinity noted in the study is further corroborated by the occurrence of electrostatic forces between the adsorbent and the adsorbate. Neutral red is a cationic dye, meaning it carries a positive charge in solution. Oxygen-doped g-C<sub>3</sub>N<sub>4</sub>, on the other hand, possesses negatively charged oxygen functional groups, which can attract the positively charged dye molecules through electrostatic forces (Xu et al., 2025). These electrostatic interactions are particularly important at higher concentrations of neutral red, where the dye molecules are more likely to come into contact with the adsorbent surface (Xu et al., 2025). The L2-type isotherm observed in the study is consistent with this type of interaction, as it suggests a significant attraction exists between the adsorbent and the adsorbate, leading to a higher adsorptive capacity (Abbasi et al., 2022; Wang et al., 2016).

The multilayer adsorption process observed in the study is another important aspect of the adsorption mechanism. In a multilayer adsorption process, the adsorbent is capable of adsorbing additional layers of adsorbate molecules on top of the initial monolayer. This is particularly significant for oxygen-doped g-C<sub>3</sub>N<sub>4</sub>, characterized by a large surface area and a mesoporous framework, which permits the stacking of several layers of dye molecules. The Sips model, which incorporates elements of both the Langmuir and Freundlich models, is well-suited to explain this type of adsorption process, as it allows for both monolayer and multilayer adsorption. The multilayer adsorption process is facilitated by the strong interactions between the adsorbate molecules themselves, as suggested by the  $\gamma$  value of 1.54 (Zhou et al., 2020). This indicates that the adsorbed neutral red molecules can interact with each other, forming additional layers on the surface of the adsorbent. These interactions could be facilitated by van der Waals forces or dipole-dipole interactions between the molecules of neutral red, which allow them to stack on top of one another in a multilayer fashion (Abbasi et al., 2022; Wang et al., 2016). The presence of these interactions is consistent with the high adsorption capacity observed in the study, as it suggests that oxygen-doped g-C<sub>3</sub>N<sub>4</sub> can continue to adsorb dye molecules even after the initial monolayer has formed.

The adsorption of neutral red onto oxygen-doped g-C<sub>3</sub>N<sub>4</sub> was most accurately represented by the Sips isotherm model, which provided the highest R<sup>2</sup> value and accurately predicted the maximum capacity of adsorption. The Sips model, blending features from both the Langmuir and Freundlich models, successfully explained the surface heterogeneity of the adsorbent and the multilayer adsorption process, making it an ideal choice for describing the adsorption behavior of oxygen-doped g-C<sub>3</sub>N<sub>4</sub>. The high adsorption affinity observed in the research can likely be attributed to the presence of chemical bonds and electrostatic forces between the adsorbent and the adsorbate, as well as interactions among the adsorbed neutral red molecules themselves (Xu et al., 2025). The multilayer adsorption process was enhanced by the extensive surface area and mesoporous structure of oxygen-doped g-C<sub>3</sub>N<sub>4</sub>, which offered ample space for the accumulation of additional layers of dye molecules. Overall, this study showcases the effectiveness of oxygen-doped g-C<sub>3</sub>N<sub>4</sub> as an adsorbent for eliminating organic pollutants like neutral red from aqueous solutions, particularly at higher concentrations of dye molecules where multilayer adsorption becomes more significant.

#### 4. Conclusions

The oxygen-doped g-C<sub>3</sub>N<sub>4</sub> (OCN), produced through a one-pot calcination method, exhibited enhanced adsorption and photocatalytic properties when in comparison to bulk g-C<sub>3</sub>N<sub>4</sub>. The swift adsorption of neutral red, achieving equilibrium in just 30 minutes, was mainly facilitated by the mesoporous structure of oxygen-doped g-C<sub>3</sub>N<sub>4</sub>, resulting in a maximum adsorptive capacity of 1.86 mg g<sup>-1</sup>—twice that of bulk g-C<sub>3</sub>N<sub>4</sub>. The pseudo-second-order model provided the best characterization of the

adsorption kinetics, implying that chemisorption is a major factor in the process. Furthermore, the photoc degradation of neutral red under visible light showed significant enhancement with oxygen-doped  $g\text{-C}_3\text{N}_4$ , achieving 86% removal compared to 51% for bulk  $g\text{-C}_3\text{N}_4$ , as a result of reduced electron-hole recombination and enhanced light absorption and. Following pseudo-first-order kinetics, the degradation rate of oxygen-doped  $g\text{-C}_3\text{N}_4$  was three times faster than that of bulk  $g\text{-C}_3\text{N}_4$ , based on the reaction rate constant. Isotherm studies revealed that the Sips model provided the best fit, indicating a multilayer adsorption process with heterogeneous active sites. Overall, the combined adsorption and photocatalytic properties of oxygen-doped  $g\text{-C}_3\text{N}_4$  make it a highly efficient material for removing neutral red from aqueous solutions, with potential applications in environmental remediation.

## Acknowledgement

The author would like to express gratitude to the Direktur Pembelajaran dan Kemahasiswaan, Kementerian Pendidikan, Kebudayaan, Riset, dan Teknologi, for their financial support in Program Kreativitas Mahasiswa bidang Riset Eksakta (PKM-RE) with Research Contract Number: 079/E2/PPK/SPPK/PKM/2024.

## References

- Abbasi, M. A., Amin, K. M., Ali, M., Ali, Z., Atif, M., Ensinger, W. & Khalid, W. 2022. Synergetic effect of adsorption-photocatalysis by GO-CeO<sub>2</sub> nanocomposites for photodegradation of doxorubicin. *Journal of Environmental Chemical Engineering*, 10(1), pp 107078.
- Gholivand, M. B., Yamini, Y., Dayeni, M. & Seidi, S. 2015. Removal of methylene blue and neutral red from aqueous solutions by surfactant-modified magnetic nanoparticles as highly efficient adsorbent. *Environmental Progress & Sustainable Energy*, 34(6), pp 1683-1693.
- Gupta, B., Gupta, A. K., Ghosal, P. S. & Tiwary, C. S. 2020. Photo-induced degradation of bio-toxic Ciprofloxacin using the porous 3D hybrid architecture of an atomically thin sulfur-doped  $g\text{-C}_3\text{N}_4/\text{ZnO}$  nanosheet. *Environmental Research*, 183(109154).
- Husein, S., Slamet & Dewi, E. L. 2024. A review on graphite carbon nitride ( $g\text{-C}_3\text{N}_4$ )-based composite for antibiotics and dye degradation and hydrogen production. *Waste Disposal & Sustainable Energy*.
- Khan, S., Noor, T., Iqbal, N. & Yaqoob, L. 2024. Photocatalytic Dye Degradation from Textile Wastewater: A Review. *ACS Omega*.
- Li, J., Qi, Y., Mei, Y., Ma, S., Li, Q., Xin, B., Yao, T. & Wu, J. 2020. Construction of phosphorus-doped carbon nitride/phosphorus and sulfur co-doped carbon nitride isotype heterojunction and their enhanced photoactivity. *Journal of Colloid and Interface Science*, 566(495-504).
- Liang, H., Zhao, J., Brouzgou, A., Wang, A., Jing, S., Kannan, P., Chen, F. & Tsiakaras, P. 2025. Efficient photocatalytic H<sub>2</sub>O<sub>2</sub> production and photodegradation of RhB over K-doped  $g\text{-C}_3\text{N}_4/\text{ZnO}$  S-scheme heterojunction. *Journal of Colloid and Interface Science*, 677(1120-1133).
- Liu, X., Ma, R., Zhuang, L., Hu, B., Chen, J., Liu, X. & Wang, X. 2021. Recent developments of doped  $g\text{-C}_3\text{N}_4$  photocatalysts for the degradation of organic pollutants. *Critical Reviews in Environmental Science and Technology*, 51(8), pp 751-790.
- Liu, Z., Zhong, Y., Hu, Z., Zhang, W., Zhang, X., Ji, X. & Wang, X. 2023. Modification of ZIF-8 nanocomposite by a Gd atom doped TiO<sub>2</sub> for high efficiency photocatalytic degradation of neutral red dye: An experimental and theoretical study. *Journal of Molecular Liquids*, 380(121729).
- Mishra, S. R., Gadore, V. & Ahmaruzzaman, M. 2024. Sustainability-driven photocatalysis: oxygen-doped  $g\text{-C}_3\text{N}_4$  for organic contaminant degradation. *RSC Sustainability*, 2(1), pp 91-100.
- Psomopoulos, C. S., Bourka, A. & Themelis, N. J. 2009. Waste-to-energy: A review of the status and benefits in USA. *Waste management*, 29(5), pp 1718-1724.

- Sadia, M., Naz, R., Khan, J., Zahoor, M., Ullah, R., Khan, R., Naz, S., Almoallim, H. S. & Alharbi, S. A. 2021. Metal doped titania nanoparticles as efficient photocatalyst for dyes degradation. *Journal of King Saud University - Science*, 33(2), pp 101312.
- Shahid, M. K., Kashif, A., Fuwad, A. & Choi, Y. 2021. Current advances in treatment technologies for removal of emerging contaminants from water – A critical review. *Coordination Chemistry Reviews*, 442(213993).
- Somnath, Ahmad, M. & Siddiqui, K. A. 2022. Synthesis of Mixed Ligand 3D Cobalt MOF: Smart Responsiveness towards Photocatalytic Dye Degradation in Environmental Contaminants. *Journal of Molecular Structure*, 1265(133399).
- Tamyiz, M. & Doong, R.-a. 2023. Synergetic effect of adsorption and photocatalysis by zinc ferrite-anchored graphitic carbon nitride nanosheet for the removal of ciprofloxacin under visible light irradiation. 21(1), pp.
- Tamyiz, M., Venkatesan, P., Thi Ngoc Anh, N., Dung Nguyen, M. & Doong, R.-a. 2023. Enhanced visible-light-responsive photodegradation of ciprofloxacin by direct Z-scheme ZnFe<sub>2</sub>O<sub>4</sub>@g-C<sub>3</sub>N<sub>4</sub> nanocomposites. *Journal of Photochemistry and Photobiology A: Chemistry*, 443(114897).
- Wang, P., Wang, X., Yu, S., Zou, Y., Wang, J., Chen, Z., Alharbi, N. S., Alsaedi, A., Hayat, T., Chen, Y. & Wang, X. 2016. Silica coated Fe<sub>3</sub>O<sub>4</sub> magnetic nanospheres for high removal of organic pollutants from wastewater. *Chemical Engineering Journal*, 306(280-288).
- Wang, S., Deng, Y., Sui, J., Hu, B., Wang, L., Che, G., Su, B., Jiang, W. & Liu, C. 2024. Reactive oxygen boosts photocatalytic oxytetracycline degradation and H<sub>2</sub>O<sub>2</sub> production by K, O and cyano co-modified carbon nitride. *Colloids and Surfaces A: Physicochemical and Engineering Aspects*, 699(134870).
- Xie, Y., Wu, J., Sun, C., Ling, Y., Li, S., Li, X., Zhao, J. & Yang, K. 2020. La<sub>2</sub>O<sub>3</sub>-modified graphite carbon nitride achieving the enhanced photocatalytic degradation of different organic pollutants under visible light irradiation. *Materials Chemistry and Physics*, 246(122846).
- Xu, Q., Fu, H., Gu, J., Lei, L. & Ling, L. 2025. Catalytic detoxification of mitoxantrone by graphitic carbon nitride (g-C<sub>3</sub>N<sub>4</sub>) supported Fe/Pd bimetallic nanoparticles. *Journal of Environmental Sciences*, 148(614-624).
- Yan, C., Yi, W., Yuan, H., Wu, X. & Li, F. 2014. A highly photoactive S, Cu-codoped nano-TiO<sub>2</sub> photocatalyst: Synthesis and characterization for enhanced photocatalytic degradation of neutral red. *Environmental Progress & Sustainable Energy*, 33(2), pp 419-429.
- Zhang, Q., Wang, B., Miao, H., Fan, J., Sun, T. & Liu, E. 2024. Efficient photocatalytic H<sub>2</sub>O<sub>2</sub> production over K<sup>+</sup>-intercalated crystalline g-C<sub>3</sub>N<sub>4</sub> with regulated oxygen reduction pathway. *Chemical Engineering Journal*, 482(148844).
- Zhou, Q., Chen, W., Jiang, X., Liu, H., Ma, S. & Wang, B. 2020. Preparation of a novel nitrogen-containing graphitic mesoporous carbon for the removal of acid red 88. *Scientific Reports*, 10(1), pp 1353.
- Zhu, J., Zhu, Y., Chen, Z., Zhao, Y. & Chen, G. 2024. Fluorine-doped TiO<sub>2</sub>/SiO<sub>2</sub>/activated carbon ternary hybrids: Enhancing adsorption and photocatalytic degradation of rhodamine B and methyl orange. *Materials Research Bulletin*, 176(112826).